



## Selective deposition of ZnO nanowires on silicon micro-pyramidal arrays



Alakananda Das<sup>a</sup>, Pushan Guha Roy<sup>a</sup>, Chirantan Singha<sup>b</sup>, Anirban Bhattacharyya<sup>a,\*</sup>

<sup>a</sup> Institute of Radio Physics and Electronics, University of Calcutta, Kolkata 700009, India

<sup>b</sup> Centre for Research in Nanoscience and Nanotechnology, University of Calcutta, Kolkata 700106, India

### ARTICLE INFO

#### Keywords:

Crystallographic wet chemical etching  
Micro-pyramids  
VLS method  
Zinc oxide nanowires  
Selective deposition of nanowires

### ABSTRACT

Growth of ZnO nanowires on various crystallographic facets of silicon was carried out in order to promote spatially-selective growth. Spontaneous growth of these structures at specific locations of a wafer is necessary for many applications, including photovoltaics and field-emission. Silicon micro-pyramidal arrays with a base of 80  $\mu\text{m}$  square and a plateau 30  $\mu\text{m}$  wide at the top were fabricated using the crystallographic wet chemical etching process. ZnO nanowires were grown onto these structures using the vapor-liquid-solid technique employing Au nanoparticles generated by annealing a sputter deposited layer. Several variations were made in the crystallographic etch process to generate different facet morphologies. Furthermore, the gold annealing step was carried out under different conditions, and its effect on the nature and density of ZnO nanowires was determined. It was observed that even for identical deposition conditions for the ZnO nanowires, modification of these two parameters strongly affected the selective deposition on various silicon facets. For relatively low Au annealing temperatures the entire surface of the micro-pyramidal structures was coated densely and uniformly with ZnO nanowires which were mostly aligned vertical to the facet surfaces. SEM as well as Cathodoluminescence (CL) imaging studies show that annealing of the Au film at higher temperature led to deposition of ZnO nanowires on the plateau at the top of the micro-pyramidal structures, while the side facets were completely bare. The nanowires deposited on the plateau on top of the pyramids were as long as 40  $\mu\text{m}$  with a diameter of  $\sim 200$  nm. CL spectra obtained from the ZnO nanowires showed clear and sharp band edge luminescence along with emission at  $\sim 500$  nm due to surface states. It is envisioned that further reduction of the plateau dimensions will lead to single nanowire deposition on top of each pyramidal structure, which is appropriate for future field-emission devices.

### 1. Introduction

Zinc Oxide (ZnO) has a wide range of applications in the field of electronic, optoelectronic, MEMS and field-emission devices [1–3]. It is a direct and wide band gap material and its large excitonic binding energy (60 meV) [4] makes it a prime candidate for high electroluminescent devices operating at elevated temperatures. ZnO nanostructures have attracted much attention over the years, and nanowires, nanorods, nanobelts, nanospheres, tetrapods and core-shell nanostructures have been reported extensively [5–7]. Many growth approaches for such structures including hydrothermal, vapor-solid (VS), vapor-liquid-solid (VLS), chemical vapor deposition (CVD), template based synthesis, etc have so far been studied [8–11].

ZnO nanowires, because of long electron diffusion length and direct and effective pathways for rapid electron transport have reaped extensive applications in the fabrication of photovoltaic devices [12–14]. Use of nanostructures also significantly enhances the optical absorption

properties of the devices by increasing the surface area and probability of multiple reflections. Such devices include not only dye-sensitized solar cells, but also quantum dot solar cells and inverted polymer solar cells [15–17]. Another important application for ZnO nanowires is in the field of electron emission, which could find its use in flat panel displays [2]. The high aspect ratio, negative electron affinity and good thermal and chemical stability of the nanowires make them important candidates for achieving high field-emission current density at a low electric field [18,19].

The major technological challenge in the development of nanowire-based electronic and optoelectronic devices, whether for optical absorption, optical emission or field emission, is the control of the uniformity, vertical orientation and alignment of the nanowires. These, along with the ability to deposit such structures controllably and selectively on to commonly used substrates is essential for technological exploitation of their very important electronic and optical properties. For use in electron emission, a large current density or large beam area

\* Corresponding author.

E-mail address: [anirban1@gmail.com](mailto:anirban1@gmail.com) (A. Bhattacharyya).

can only be achieved if the nanowires are in the form of vertical arrays. For optical absorption based applications such as solar cells, however, the nanowires should cover the entire surface area of the device. Thus it is necessary to controllably deposit ZnO nanowires on a commonly used substrate like silicon, either at specific locations, or to cover the entire device area, depending on the application. This must also be achievable at a reasonable cost. Hydrothermal, VS, or VLS processes are essentially low cost, but the nanowires developed are usually randomly oriented and there is no easy method for spatially restricting their growth. Several groups have reported the use of electron beam lithography to produce position-controlled nanowire arrays [20,21]. However, this method is complex, expensive and time consuming. Similarly, use of templates of various forms [22–24] has also been reported, but add many process steps thereby making them less cost effective.

In this paper we have investigated the growth of ZnO nanowires by VLS method on to various crystalline facets of silicon in order to achieve spatial selectivity.

## 2. Methods

The growth of ZnO nanowires was carried out using the vapor-liquid-solid (VLS) process on to silicon [orientation (100), 4-in. diameter, thickness  $500 \pm 25 \mu\text{m}$ , B doped, p-type  $1\text{--}10 \Omega\text{-cm}$ ] substrates. These substrates were coated with a thermal  $\text{SiO}_2$  layer,  $2 \mu\text{m}$  thick on both sides of the wafer. Crystallographic wet chemical etch was carried out on these substrates to generate pyramidal facets, using process steps described schematically in Fig. 1.

The wafers were cleaned using trichloroethylene, acetone, isopropyl alcohol and DI water. Subsequently the  $\text{SiO}_2$  layer was lithographically patterned to form square features of  $80 \times 80 \mu\text{m}$  in size (Fig. 1b). This was carried out using a MA6-BA6 Mask Aligner (Suss Microtec), S1813 photoresist and MF26A developer (Shipley). Care was taken to align the edge of the box like structures along the [100] direction. The  $\text{SiO}_2$  layer was then selectively etched using a buffer oxide etch (BOE) solution at room temperature, generating an etch rate of  $0.83 \text{ nm/s}$  (Fig. 1c).

After removing the photoresist, the samples were etched in KOH solution (35 g KOH pellets in 190 ml DI water) at  $80^\circ\text{C}$ , while continuously stirring. An etch rate of up to  $8.89 \text{ nm/s}$  was achieved in the vertical direction. The selectivity of etch of (100) planes over (111) planes was further enhanced by the use of isopropyl alcohol at 1:5 ratio with the KOH solution. Undercutting of the  $\text{SiO}_2$  “box” structures were observed and arrays of nearly pyramidal structures bound by the (111) planes were obtained (Fig. 1d). After removal of the  $\text{SiO}_2$  layer, this was then employed as the template on to which ZnO nanowires were deposited using VLS techniques.

Gold (Au) thin films of thickness  $1\text{--}3 \text{ nm}$  were then deposited on to the samples by the sputter deposition technique using a Quorum (Q150T ES) sputter coater. Annealing of the deposited film was carried out at  $900\text{--}950^\circ\text{C}$  in a tube furnace under inert argon (Ar) ambience for

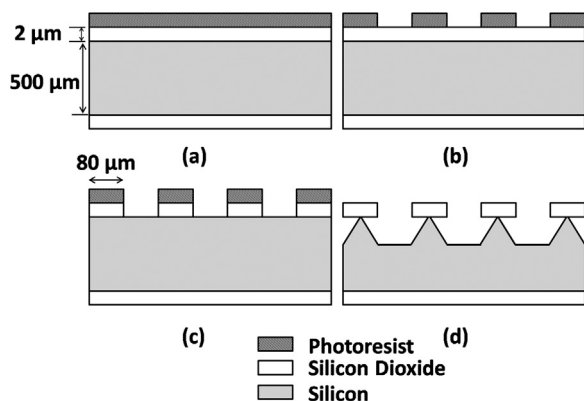


Fig. 1. Fabrication steps for Silicon micro-pyramidal structures.

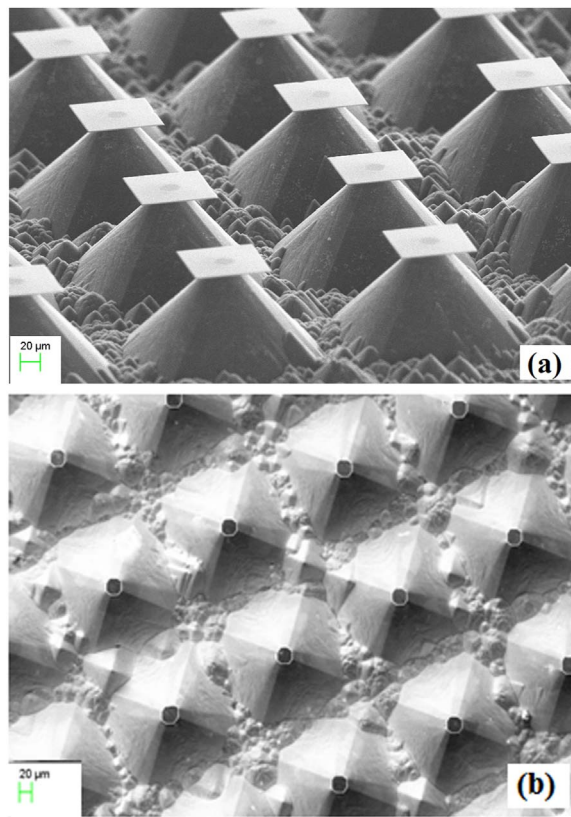


Fig. 2. SEM image of the silicon micro-pyramidal structures: (a) after crystallographic etch step and (b) after removal of the  $\text{SiO}_2$  layer to reveal the plateau region.

30 min under atmospheric pressure. This step was employed for the formation of Au nanoparticles. Equal amounts of ZnO and graphite powders were mixed and the mixture was placed in a quartz boat kept at  $900^\circ\text{C}$  in a two zone tube furnace. The annealed Au-coated faceted silicon substrates were placed downstream and were maintained at  $800\text{--}850^\circ\text{C}$ . Argon was used as the carrier gas and the flow rate was controlled between 3 and 5 sccm. The reaction was carried out for 30 min under atmospheric pressure.

The surface morphology of the films was examined using scanning electron microscopy (ZEISS, EVO18 and JEOL JSM-7600F). A GATAN MonoCL4 system mounted on the JEOL FESEM was used for room temperature Cathodoluminescence imaging and spectroscopy measurements.

## 3. Results and discussions

The micro-pyramidal structures, after the crystallographic etch process were observed using scanning electron microscopy (SEM), and the image is presented in Fig. 2(a). The under-etching below the oxide layer ( $80 \mu\text{m}$  square) can be clearly seen. Subsequent removal of the  $\text{SiO}_2$  layer using a Buffer Oxide Etch solution at room temperature for 30 min reveals a  $30 \mu\text{m}$  wide top plateau as seen in Fig. 2(b). This dimension can be controlled by modifying the KOH etch process endpoint, and can be completely eliminated, revealing a pointed pyramidal structure, as has been carried out for some samples. The sidewalls of the pyramids can be chosen to be either smooth and clearly defined, or faceted and stepped by modifying the etch process, specifically the amount of isopropanol employed. Complex facets can also be generated by rotating the orientation of the  $\text{SiO}_2$  squares with respect to the in plane [100] direction. In this work however, we have focused on the smooth and stepped pyramidal structures exclusively.

Growth of ZnO nanowires on to the micro-pyramidal structures was carried out by VLS method, using Au nanoparticles. The details of the

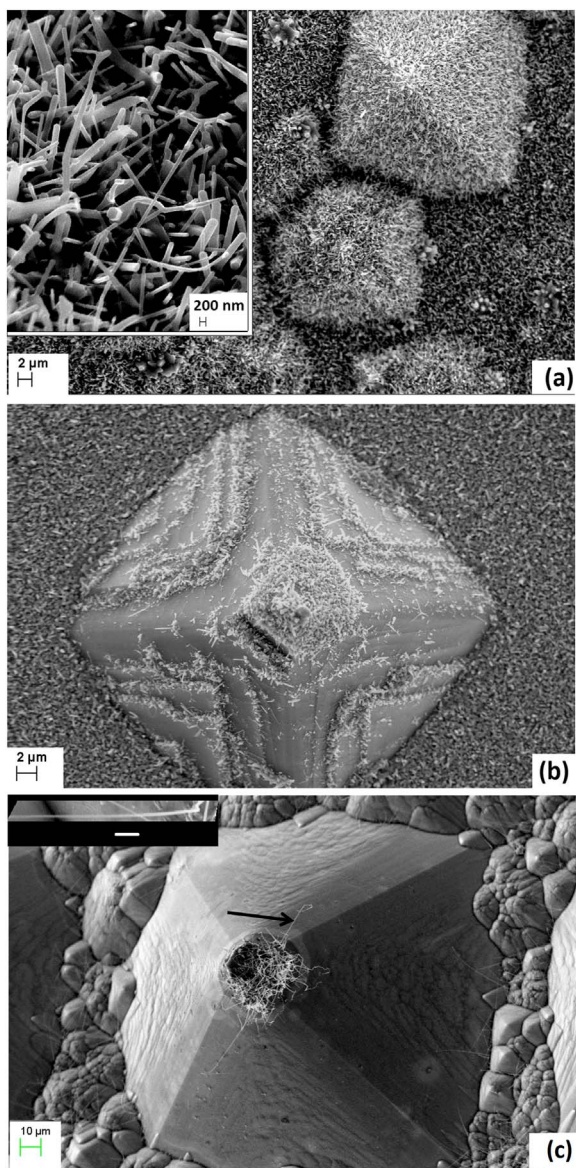


**Fig. 3.** SEM images showing the variation of ZnO nanowire distribution for samples S1 (a), S2 (b) and S3 (c). Inset in (a) shows the ZnO nanowires in high magnification. Inset in (c) shows part of a very long nanowire deposited on top of the micro-pyramid (bar size 1  $\mu\text{m}$ ).

nanowire formation on to flat silicon substrates and on to ZnO thin films have been reported previously [25]. The deposition of thin Au film and subsequent annealing generates the nanoparticles, whose density is typically a function of the thickness of the film and the annealing temperature. In this case however, an additional parameter is the surface morphology of the silicon, specifically the crystal planes on to which the nanoparticles are formed.

The ZnO nanowires formed by the VLS process have been extensively investigated by SEM and the results are presented in Fig. 3. As can be clearly seen, the coverage and the density vary strongly for the three samples S1, S2 and S3.

For all three samples, the sputter deposition condition for Au thin film was identical. Furthermore, the growth conditions for ZnO nanowires were nominally the same for all three samples, and the temperature profile, argon flow rate, and ZnO/graphite mixture were identical. The sole variation among the samples was the temperature of annealing of the Au thin film, which was 900 °C for sample S1, and 950 °C for the samples S2 and S3. This modification of annealing

temperature however is expected to strongly affect the formation i.e. the density, size, and spatial distribution of the Au nanoparticles.

It was observed from SEM images that for sample S1 (Fig. 3a), the surface is completely covered with ZnO nanowires, with a very high density. The nanowires are mostly vertical to the deposition surface, as can be seen from the inset of Fig. 3a. While it is difficult to clearly measure the average height due to the vertical orientation of the nanowires, it can be estimated to be about 1.2  $\mu\text{m}$ . There is however a variation in thickness from 100 nm to less than 400 nm. Again, it should be stressed that for this sample S1 the entire surface of the pyramids, as well as the base region between the pyramids are completely coated with ZnO nanowires.

For the samples S2 and S3, all conditions for the deposition of ZnO nanowires were nominally identical. The annealing temperature for Au thin films for both these samples was 950 °C, which is significantly higher than that used for sample S1. However, the surface morphology of the underlying faceted silicon was deliberately varied, in order to understand its effect on the final density of nanowire growth. In case of sample S2, the sidewalls of the micro-pyramids were chosen to be faceted with clearly defined steps, by modifying the amount of isopropanol in the crystallographic etch solution. The sidewalls of sample S3, on the other hand was kept completely smooth.

It can be clearly observed from the SEM images that for the sample S2, ZnO nanowires are deposited mostly at the stepped facets of the sidewalls, while the sloped faces are almost clear (Fig. 3b). For sample S3, there are no stepped facets and all the pyramidal faces are completely devoid of nanowires (Fig. 3c). On the other hand, the plateaus on the top of the micro-pyramidal structures for both the samples are completely covered with ZnO nanowires. Another important feature that can be observed is that while for sample S1 and for similar samples where ZnO nanowires were deposited on to silicon substrates, the average nanowire height was about 1.2  $\mu\text{m}$ , for sample S3 extremely long nanowires with length up to 40  $\mu\text{m}$  were formed. Here the aspect ratio was determined to be 40  $\mu\text{m}$  to 200 nm. In this case such structures may be termed as micro/nanowires. Only a part of such a typical nanowire is shown in the inset of Fig. 3c. In addition to the nanowires on top of the plateau, nanowires with high density were also observed at between the pyramids, but the pyramidal faces are completely bare.

The quality of the nanowires formed was investigated by room temperature cathodoluminescence (CL) panchromatic imaging and spectroscopy. We compare the luminescence properties of nanowires grown on the plateau on top of the micro-pyramidal structures, to those deposited between the pyramids, which are essentially similar to nanowires deposited on to silicon wafers by standard VLS process. Such nanowires have been extensively studied previously, and show excellent excitonic peaks in the low temperature PL spectra [25].

Fig. 4b shows the CL image of sample S3. The corresponding FESEM image of the micro-pyramidal structures is presented in Fig. 4a for easy identification of the luminescence generated from ZnO nanowires grown on the top plateau (indicated by the arrows in Fig. 4b) and that generated by ZnO nanowires on the base of the substrate. Again, the absence of any ZnO nanowires on the pyramid facets is clearly observed from the totally dark regions around pyramid summit.

CL spectra were taken at higher SEM magnification so that luminescence exclusively obtained from the nanowires on the top of the plateau can be compared with those from the base of the pyramid. The spectra, as seen in Fig. 5 are fundamentally similar, with a band-edge luminescence at around 380 nm and a broad sub-bandgap luminescence that peaks around 500 nm which has been attributed in the literature to the surface defect states [26]. From the sharp band-edge peak, it can be concluded that these nanowires are of high structural quality, with few defect states, except for those arising from the very high surface to volume ratio. These defect states increase with an increase of the length of the nanowire. From SEM images it is already proven that the nanowires at the top of the plateau are significantly longer than those grown at the base, which leads to a higher surface to volume ratio and hence a

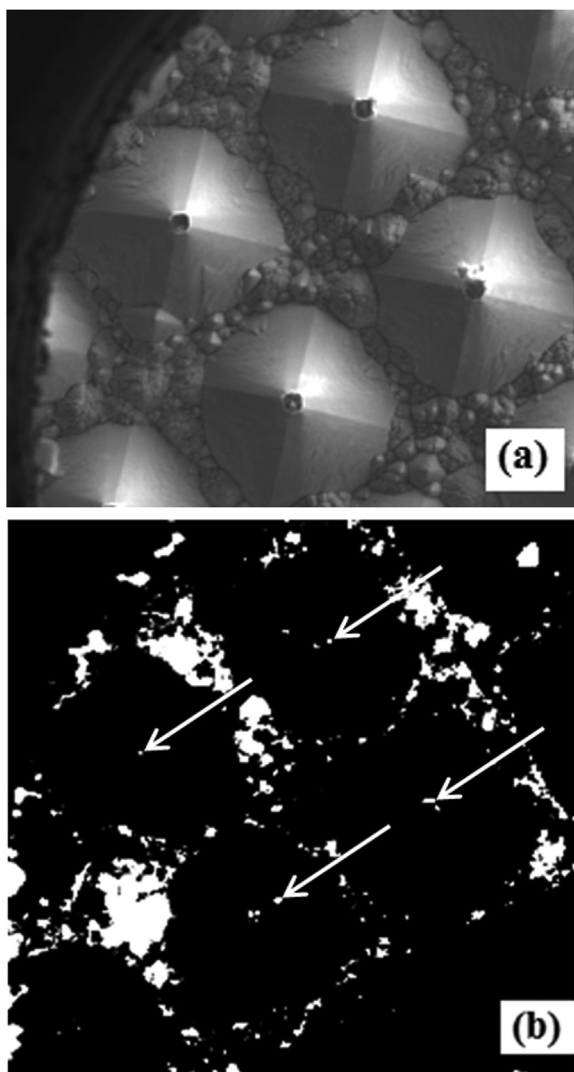


Fig. 4. FESEM (a) and CL image (b) clearly showing the positioning of the nanowires only at the base and the top plateau (shown by arrows) of the micro-pyramidal structures.

larger number of defect states. This is the reason behind the higher relative intensity of the sub-bandgap luminescence compared to the band-edge luminescence of the nanowires deposited at the plateau on top of the pyramids (Fig. 5b). The higher noise in Fig. 5b is due to the weaker signal coming from the few nanowires at the top of the plateau. More detailed measurements are necessary to evaluate luminescence from single nanowires.

The fundamental growth mechanism for the selective deposition of the nanowires on top of the plateau compared to the sloped facets remains to be discussed. There can be several possible mechanisms that may lead to this selectivity.

The initial step, i.e. the formation of the crystal planes by wet chemical etching process, may lead to different surface morphology on the sidewalls, and on the top of the plateau. For sample S3, the sidewalls are shown to be very flat. The top of the plateau, specially the edge “rim” is rough at the nanometer scale due to random fluctuations of the etch process. The area between the pyramids is also relatively rough. When the gold film is deposited and then annealed, surface features such as roughness, pitting, etc can reduce surface diffusivity of the gold. Longer surface diffusion lengths lead to large gold particles during annealing at high temperature due to the process of aggregation [27]. Thus, the droplet size is smaller on the rough top surface and the region between the pyramids than on the smooth facets for sample S3.

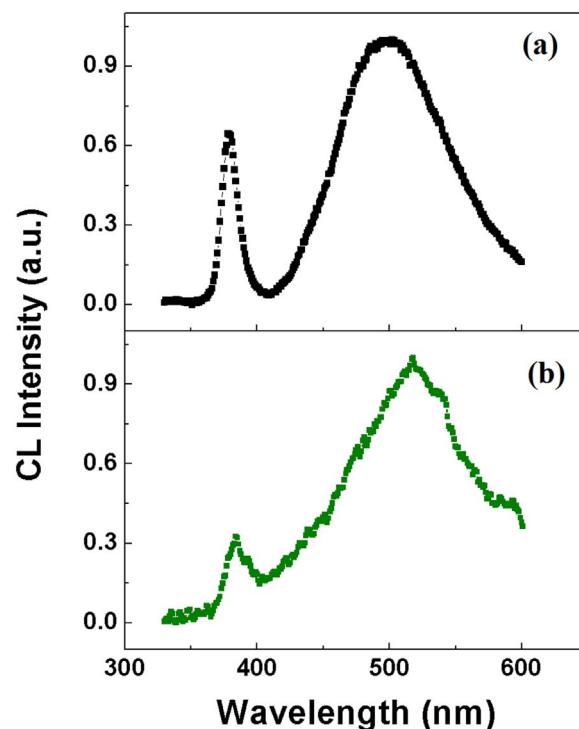


Fig. 5. CL spectra from the nanowires at the base (a) and top (b) of the micro-pyramidal structures.

For sample S2, the pyramid sidewalls have both extend smooth regions as well as short “ledge” like features. In this case also, the gold nanoparticles will be small on these ledges than on the smooth surfaces. For sample S1, since the annealing temperature is low, the particle size is small throughout.

During the nanowire growth stage, for gold aggregates with relatively large size, the possibility of supersaturation is low and nanowires are not formed [28]. However, for smaller gold nanoparticles present on the top plateau of S2 and S3, on the ledges of sample S2 and the rough region between pyramids, nanowires are clearly visible. Under this mechanism, the variation of the diffusion length of gold creates the selectivity of the nanowire deposition.

The very long nanowires formed on the top of the pyramids of sample S3 can be due to the local variation of carrier gas speed and the precursor concentrations. ZnO is converted to Zn by the graphite, which travels in the vapor state downwind with the argon, till it deposits by the VLS process by dissolution in the Au nanoparticle and reacting with the carbon monoxide formed from the breakdown of ZnO to Zn by carbon in the first step. This flow rate is low at the base between the pyramids, and is the highest for the plateau at the top. This, along with the fact that ZnO nanowires are formed only at the apex for sample S3, generates nanowires as long as 40  $\mu\text{m}$  as can be seen in Fig. 3c.

#### 4. Conclusions

In this work we have achieved spatial selective deposition of ZnO nanowires on to various crystalline facets of silicon. Well defined arrays of silicon micro-pyramids, each with a small but well defined plateau on the top were generated using crystallographic wet chemical etch. The ZnO nanowires were deposited on to the facets using the VLS process, employing Au nanoparticles formed by high temperature annealing of a sputter deposited Au thin film.

It was observed that when this annealing process was carried out at relatively lower temperature, the entire surface of the pyramidal structures was coated uniformly with ZnO nanowires with high density, mostly aligned vertical to the facet surfaces. This type of structure is

expected to lead to efficient light trapping in solar cells. However, for higher annealing temperatures of the Au thin films, the final ZnO nanowires are deposited at the plateau on top of the micro-pyramids while the sidewalls are completely void of any nanowires or ZnO thin films, a fact which has been verified using CL imaging. In addition, the nanowires deposited on top of the pyramids are as long as 40  $\mu\text{m}$  with a diameter of  $\sim 200$  nm. CL spectroscopy indicated that the nanowires have good optical characteristics with a clear and sharp band-edge emission, along with deep levels generated due to the very high surface to volume ratio. Controlled reduction of the plateau size will progressively reduce the number of ZnO nanowires, till a single nanowire can be positioned on top of each micro-pyramidal structure. Such selective deposition of ZnO nanowire arrays, without the need for electron-beam lithography, could pave the way for future cost-effective field-emission devices.

### Acknowledgements

The authors would like to acknowledge Pratyush Sengupta for SEM and Samrat Kundu for FESEM and CL imaging and spectroscopy. Alakananda Das (09/ 028 (0946)/2015-EMR-I) would like to acknowledge the Council of Scientific and Industrial Research (CSIR) Senior Research Fellowship scheme and Chirantan Singha would like to acknowledge the Department of Science and Technology (DST) INSPIRE fellowship (IF120257) for funding their respective work. We are also grateful to Sayantani Sen, Pallabi Pramanik, Arpita Das and Suchismita Paul for their invaluable help and advice.

### References

- [1] N.H. Nickel, E. Terukov, *Zinc Oxide-a Material for Micro-and Optoelectronic Application*, Springer, Netherlands, 2005.
- [2] C.J. Lee, T.J. Lee, S.C. Lyu, Y. Zhang, H.J. Lee, *Appl. Phys. Lett.* 81 (2002) 3648–3650.
- [3] Z.L. Wang, J. Song, *Science* 312 (2006) 242–246.
- [4] A. Janotti, C.G. Van de Walle, *Rep. Prog. Phys.* 72 (2009) 126501.
- [5] C. Jagadish, S.J. Pearton, *Zinc Oxide Bulk, Thin Films, and Nanostructures: Processing, Properties and Applications*, Elsevier, New York, 2006, p. 339.
- [6] M.C. Newton, P.A. Warburton, *Mater. Today* 10 (2007) 50–54.
- [7] D.G. Tong, P. Wu, P.K. Su, D.Q. Wang, H.Y. Tian, *Mater. Lett.* 70 (2012) 94–97.
- [8] S.Y. Li, C.Y. Lee, T.Y. Tseng, *J. Cryst. Growth* 247 (2003) 357–362.
- [9] P.C. Chang, Z. Fan, D. Wang, W.Y. Tseng, W.A. Chiou, J. Hong, J.G. Lu, *Chem. Mater.* 16 (2004) 5133–5137.
- [10] B. Liu, H.C. Zeng, *J. Am. Chem. Soc.* 125 (2003) 4430–4431.
- [11] G. Cao, D. Liu, *Adv. Colloid Interface* 136 (2008) 45–64.
- [12] Q. Zhang, G. Cao, *Nano Today* 6 (2011) 91–109.
- [13] T.R. Chetia, D. Barpuzary, M. Qureshi, *Phys. Chem. Chem. Phys.* 16 (2014) 9625–9633.
- [14] S. Ren, N. Zhao, S.C. Crawford, M. Tambe, V. Bulovic, S. Gradecak, *Nano Lett.* 11 (2011) 408–413.
- [15] I.J. Kramer, E.H. Sargent, *ACS Nano* 5 (2011) 8506–8514.
- [16] O.E. Semonin, J.M. Luther, S. Choi, H.Y. Chen, J. Gao, A.J. Nozik, M.C. Beard, *Science* 334 (2011) 1530.
- [17] C.E. Small, S. Chen, J. Subbiah, C.M. Amb, S.W. Tsang, T.H. Lai, J.R. Reynolds, F. So, *Nat. Photonics* 6 (2012) 115–120.
- [18] D. Banerjee, S.H. Jo, Z.F. Reng, *Adv. Mater.* 16 (2004) 2028–2032.
- [19] Y.K. Tseng, C.J. Huang, H.M. Cheng, I.N. Lin, K.S. Liu, I.C. Chen, *Adv. Funct. Mater.* 13 (2003) 811–814.
- [20] H.T. Ng, J. Han, T. Yamada, P. Nguyen, Y.P. Chen, M. Meyyappan, *Nano Lett.* 4 (2004) 1247–1252.
- [21] Z. Li, S. Butun, K. Aydin, *ACS Nano* 8 (2014) 8242–8248.
- [22] A.M. Munshi, D.L. Dheeraj, V.T. Fauske, D.C. Kim, J. Huh, J.F. Reinertsen, L. Ahtapodov, K.D. Lee, B. Heidari, A.T.J. van Helvoort, B.O. Fimland, H. Weman, *Nano Lett.* 14 (2014) 960–966.
- [23] C.Y. Nam, A. Stein, K. Kisslinger, C.T. Black, *Appl. Phys. Lett.* 107 (2015) 203106.
- [24] F. Grote, R.S. Kuhnel, A. Balducci, Y. Lei, *Appl. Phys. Lett.* 104 (2014) 053904.
- [25] P.G. Roy, A. Dutta, A. Das, S. Sen, P. Pramanik, A. Bhattacharyya, *Mater. Res. Express* 2 (2015) 075007.
- [26] I. Shalish, H. Temkin, V. Narayanamurti, *Phys. Rev. B* 69 (2004) 245401.
- [27] K. Nagashima, T. Yanagida, H. Tanaka, T. Kawai, *Appl. Phys. Lett.* 90 (2007) 233103.
- [28] T. Yanagida, K. Nagashima, H. Tanaka, T. Kawai, *J. Appl. Phys.* 104 (2008) 016101.